

# Control Strategies for Hard-Disk Spindle Drives

T.S. Low\*, C. Bi\*\*, K.T. Chang\* and C.S. Soh\*

\*Magnetics Technology Centre, National University of Singapore, Singapore

\*\*Western Digital (S) Pte Ltd, Singapore

**Abstract** This paper describes the development of a control strategy for high-torque spindle motor drives used in hard-disk drives (HDDs). It uses the per-phase torque characteristics of the motor, which is termed the motor *identity*, for the optimization of the input current to achieve high efficiency and optimal torque production. This control strategy is described as 'Identity Control'. A self-starting technique is also developed to start the spindle motor and to operate the motor without sensors. This paper also discusses the implementation of a zero voltage switching quasi resonant converter (ZVS-QRC) to achieve high power efficiency by minimizing switching losses in the power devices. Simulation and experimental results are presented and a comparison is made for the identity controlled spindle drive and a BLDCM controlled spindle drive.

## 1. INTRODUCTION

Permanent magnet synchronous motors (PMSMs) are currently used in many high-performance speed and position controlled applications. They are now widely used as spindle motors in HDDs, in the form of brushless dc motor (BLDCM) mode, as they have many desirable features such as high torque to inertia ratio, sealed configuration and simple control. However, the reduction in the formats and increasing areal data storage density of HDDs present several challenging issues in spindle motor design to be addressed due to the space constrain, run-out requirement, torque ripple demand, acoustic noise generation and bearing selection.

Spindle motors in HDDs are often operated with indirect sensing so as to enhance reliability and to achieve further reduction in the size of the overall drive system. One popular method is to sense the position of the rotor from the zero crossings of the back-emf [1]. However, with the use of indirect sensing method no position information is available at starting and an additional circuitry has to be incorporated to start the motor. Chip manufacturers have integrated both sensorless and self-starting features in a single IC chip [1], however, careful tuning of the chip is required before the chip can be properly used to start the motor.

This paper reports a few strategies for an efficient, high-torque spindle motor drives which also possesses easy self-starting capability and that can operate without any position sensor. These control techniques are also coupled with a quasi resonant power converter to achieve a higher level of efficiency.

The hardware implementation of the hard-disk spindle drive and control system comprising the identity controller, open-loop frequency controller and ZVS-QRC is described. A comparative study with a conventional sensorless, BLDCM mode operated spindle drive and with conventional PWM power supply converter is performed.

## 2. MODELING OF DISK-DRIVE SPINDLE MOTORS

The spindle motors in HDDs are basically permanent-magnet synchronous motor (PMSM) and they can be modeled using one of several available mathematical models [8]. In this section, the voltage and torque equations of the PMSM are modeled using the *abc* model.

### 2.1 Voltage Equations

The *abc* model [4] of the three-phase PMSM spindle motor is illustrated in Figure 1. In this model, three phase windings and the fictitious field winding of the motor are modeled as four series connections of resistance and inductances.

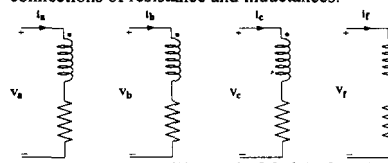


Fig 1. abc Model of PMSM

From the model, the voltage equation for the motor is,

$$\begin{bmatrix} v_a \\ v_b \\ v_c \end{bmatrix} = R \begin{bmatrix} i_a \\ i_b \\ i_c \end{bmatrix} + \frac{d}{dt} \begin{bmatrix} \lambda_a \\ \lambda_b \\ \lambda_c \end{bmatrix} \quad (2-1)$$

where  $R$  is the phase resistance,  $i$  is the phase current and  $\lambda$  is the phase flux linkage

The flux linkages are given as

$$\begin{bmatrix} \lambda_a \\ \lambda_b \\ \lambda_c \\ \lambda_f \end{bmatrix} = \begin{bmatrix} L_a & M_{ab} & M_{ac} & M_{af} \\ M_{ba} & L_b & M_{bc} & M_{bf} \\ M_{ca} & M_{cb} & L_c & M_{cf} \\ M_{fa} & M_{fb} & M_{fc} & L_f \end{bmatrix} \begin{bmatrix} i_a \\ i_b \\ i_c \\ i_f \end{bmatrix} \quad (2-2)$$

where  $L$  is the self inductance of winding and  $M_{xy}$  is the mutual inductance between coil  $x$  and  $y$ . Inductances are functions of electrical position,  $\theta$ , and they can be expressed as Fourier functions of  $\theta$ .

In a symmetrical and balanced machine, only one phase in the motor needs to be considered in mathematical manipulations and analysis. The remaining two phases will have the same voltage equations delayed by  $2\pi/3$  and  $4\pi/3$  respectively. Thus, only the electrical equation for phase A is considered and it is written as follows,

IEEE Catalogue No. 95TH8025

0-7803-2423-4/95/\$4.00©1995 IEEE

$$v_a = i_a R + i_a \omega_e \frac{dL_a}{d\theta} + i_b \omega_e \frac{dM_{ab}}{d\theta} + i_c \omega_e \frac{dM_{ac}}{d\theta} + L_a \frac{di_a}{dt} + M_{ab} \frac{di_b}{dt} + M_{ac} \frac{di_c}{dt} + i_f \omega_e \frac{dM_{af}}{d\theta} \quad (2-3)$$

where  $\omega_e$  is the frequency of the supply. All the terms in eqn. 2-3 are armature currents ( $i_a$ ) dependent, except for the last term in the equation. The last term is the back emf of the motor and its magnitude is proportional to the rate of change of the flux linkage produced by the permanent magnet.

HDD spindle motor uses cylindrical rotor and therefore the mutual inductances and stator self inductances are not functions of the position,  $\theta$  [2]:

$$\frac{dL_x}{d\theta} = 0 \quad \text{and} \quad \frac{dM_{xy}}{d\theta} = 0 \quad (2-4)$$

In addition, by assuming a symmetrical structure,

$$L = L_a = L_b = L_c \quad (2-5)$$

$$M = M_{ab} = M_{bc} = M_{ca}$$

Moreover, due to the absence of neutral line in disk drive spindle motors,

$$i_a + i_b + i_c = 0 \quad (2-6)$$

the voltage equation can be further simplified to

$$v_a = i_a R + (L - M) \frac{di_a}{dt} + i_f \omega_e \frac{dM_{af}}{d\theta} \quad (2-7)$$

The corresponding voltage equation for phases B and C are as follows:

$$v_b = i_b R + (L - M) \frac{di_b}{dt} + i_f \omega_e \frac{dM_{bf}}{d\theta} \quad (2-8)$$

$$v_c = i_c R + (L - M) \frac{di_c}{dt} + i_f \omega_e \frac{dM_{cf}}{d\theta} \quad (2-9)$$

## 2.2 Torque Equations

Using the energy method based on the principle of conservation of energy [8], the torque that is developed by the motor is given by

$$T_m = \left. \frac{\partial \sum [\lambda i]}{\partial \theta_m} \right|_{i=\text{const}} \quad (2-10)$$

From Eqn. (2-2), the above differentiation results the following:

$$\sum \lambda i = i_f^2 L_f + i_a^2 L_a + i_b^2 L_b + i_c^2 L_c + 2i_a i_b M_{ab} + 2i_b i_c M_{bc} + 2i_c i_a M_{ca} + 2i_a i_f M_{af} + 2i_b i_f M_{bf} + 2i_c i_f M_{cf} \quad (2-11)$$

By denoting the pole number of the machine as  $p$ , the relationship between the electrical angle ( $\theta$ ) and mechanical angle ( $\theta_m$ ) is,

$$\theta = p \theta_m / 2 \quad (2-12)$$

Substituting Eqn. 2-11 and Eqn. 12 into Eqn. 2-10, the motor torque developed is given by

$$T_m = T_{cx} + T_a + T_b + T_c$$

where

$$T_a = \frac{p}{2} \left\{ \frac{1}{2} \left( i_a^2 \frac{dL_a}{d\theta} + i_a i_b \frac{dM_{ab}}{d\theta} + i_a i_c \frac{dM_{ac}}{d\theta} \right) + i_a i_f \frac{dM_{af}}{d\theta} \right\}$$

$$T_b = \frac{p}{2} \left\{ \frac{1}{2} \left( i_b^2 \frac{dL_b}{d\theta} + i_a i_b \frac{dM_{ab}}{d\theta} + i_b i_c \frac{dM_{bc}}{d\theta} \right) + i_b i_f \frac{dM_{bf}}{d\theta} \right\}$$

$$T_c = \frac{p}{2} \left\{ \frac{1}{2} \left( i_c^2 \frac{dL_c}{d\theta} + i_a i_c \frac{dM_{ac}}{d\theta} + i_b i_c \frac{dM_{bc}}{d\theta} \right) + i_c i_f \frac{dM_{cf}}{d\theta} \right\}$$

$$T_{cx} = \frac{p}{2} \left\{ \frac{1}{2} \left( i_f^2 \frac{dL_f}{d\theta} \right) \right\} \quad (2-13)$$

The above equations describe the torque produced by a PMSM in terms of the excitation and reluctance torques [2]. In the A-phase torque in eqn (2-13), the first three components are reluctance torque components, and the last term being the excitation torque component. The reluctance torque arises from reluctance (or inductance) variations due to motor saliencies. Excitation torque is the result of the interaction between the airgap flux and the stator excitation; and it is the tendency of the excited rotor to align with the excited stator and this torque can only exist in a doubly excited machine. In addition to these two components, there exists a subclass of reluctance torque, known as cogging torque,  $T_{cg}$ , which is caused by the variation of the self reluctance of the field coil. This variation of self reluctance of the field coil is caused by the geometric structure of the stator. The presence of slots on the stator causes the self reluctance of the field coil to vary with rotor position.

The mutual and self inductances in a HDD spindle motor are independent from the rotor position, as indicated in eqn (2-14). All reluctance torque components in eqn (2-13) are therefore ignored and the torque components in eqn (2-13) are reduced to the following:

$$T_a = \frac{p}{2} \left\{ i_a i_f \frac{dM_{af}}{d\theta} \right\}, \quad T_b = \frac{p}{2} \left\{ i_b i_f \frac{dM_{bf}}{d\theta} \right\}, \quad T_c = \frac{p}{2} \left\{ i_c i_f \frac{dM_{cf}}{d\theta} \right\} \quad (2-14)$$

## 2.3 Motor Dynamic Equation

The motor dynamic equation, which relates the electrically developed torque to the mechanical performances, is given by eqn (2-15):

$$T_m = J\alpha + B\omega + T_L \quad (2-15)$$

where  $T_m$  is the electromagnetic torque developed by the motor,  $J$  is the total inertia of the motor and load,  $\alpha$  is the acceleration experienced by the rotor shaft,  $B$  is the damping coefficient of the shaft,  $\omega$  is the angular velocity of the shaft and  $T_L$  is the load torque.

Equations 2-7 to 2-9, 2-14 and 2-15 describe both the electromagnetic and mechanical subsystems and they form the complete mathematical model of disk-drive spindle motor.

## 3. IDENTITY CONTROL FOR SPINDLE MOTORS

### 3.1 Concept of Identity Control

Hard-disk spindle motors are currently being driven using voltage control where the voltage input excitation to the stator windings are of rectangular shape of width  $120^\circ$ . This voltage excitation is aimed at achieving rectangular shaped phase currents by assuming that the back emf of the motor is rectangular/trapezoidal and its inductance is negligible. These two assumptions are needed

for a simple and cheap control system for the spindle drives. However, in most motors these two assumptions are not true. As a result the torque per unit current of the motor is not maximized. To improve this index, a novel method, *Identity Control*, is proposed to maximize the torque per unit current of the motor.

Identity Control is an optimal torque control strategy first by proposed by Bi, Chang and Low [3] in the control applications using PMSMs. This torque control method is novel in the sense that the control does not take the conventional motor parameters into consideration, instead, the motor is now characterized by its *identity* and this identity contains all the necessary information for the construction of a current controlled torque controller. Based on the motor identity, the identity control algorithm produces an optimal current to the motor that will attain certain torque performance. In a previous study [4], the theory of identity control has been described and the related lemmas proven. It was applied for the minimization of torque pulsation in a current-controlled PMSM drive, in order to achieve a ripple-free smooth torque output. In the application of this technique to HDD spindles, it will be used to maximize the torque output per unit current.

### 3.2 The Identity for HDD Spindle Motors

The A-phase identity,  $\tau_a$ , is defined to be the torque position profile [3, 4], that is obtained by setting the phase currents  $i_a = 1A$  and  $i_b = i_c = 0$  and it is given by

$$\tau_a = i_f \frac{dM_{af}}{d\theta} \quad (3-1)$$

A comparison with the phase-A voltage equation, Eqn. 2-7, shows that the identity of the spindle motor appears in the last term of the phase-A voltage equation. In fact, this last term constitutes the back-emf of the motor. Thus, the identity of the hard-disk spindle motor can be obtained from the back emf of the motor where

$$v_a|_{i_a=0} = Emf_a = i_f \omega \frac{dM_{af}}{d\theta} \quad (3-2)$$

and

$$\tau_a = \frac{Emf_a}{\omega} \quad (3-3)$$

The identity can thus be determined by extracting the motor back-emf experimentally. Ignoring the harmonics higher than the 5th, the identity can then be Fourier analyzed to give the following equations:

$$Emf_a = Emf_1 \sin \theta + Emf_5 \sin 5\theta \quad (3-4)$$

The third harmonic component is non-existent from the above equation as the spindle motor is a three-phase motor.

### 3.3 Derivation of Identity Current For Spindle Motors

In the context of spindle motor, the identity current is the optimum current excitation that will produce the maximum output torque, or equivalently, the optimum current that will produce least copper and inverter loss.

From eqns. (3-3) and (3-4), the identity of the motor can be written as follows:

$$\tau_a = \tau_{a1} \sin \theta + \tau_{a5} \sin 5\theta \quad (3-5)$$

and the phase-A torque takes the form,

$$T_a = \frac{P}{2} i_a \left\{ \tau_{a1} \sin \theta + \tau_{a5} \sin 5\theta \right\} \quad (3-6)$$

where

$$i_a = \sum_{n=0, n \neq 3k}^{\infty} i_{an} \sin(n\theta - \varphi_n)$$

Clearly, the ideal current would have  $\varphi_n = 0$  and  $i_{an} = 0$  for  $n \neq 1, 5$ . That is, the injected currents should be in phase with the motor identity. Currents harmonics of order other than the first and the fifth, which do not contribute to the useful torque, should be made zero. Hence, the injected current is reduced to the following form,

$$i_a = i_{a1} \sin \theta + i_{a5} \sin 5\theta \quad (3-7)$$

Consequently, the A-phase torque is rewritten as

$$\begin{aligned} T_a &= \frac{P}{2} \left\{ i_{a1} \sin \theta + i_{a5} \sin 5\theta \right\} \left\{ \tau_{a1} \sin \theta + \tau_{a5} \sin 5\theta \right\} \\ &= \frac{P}{2} \left\{ \frac{i_{a1} \tau_{a1} + i_{a5} \tau_{a5}}{2} \right\} - \frac{P}{2} \left\{ \frac{i_{a1} \tau_{a5} + i_{a5} \tau_{a1}}{2} \right\} \cos 6\theta \\ &= -\frac{P}{2} \left\{ \left( \frac{i_{a1} \tau_{a1} + i_{a5} \tau_{a5}}{2} \right) \cos 2\theta + \left( \frac{i_{a1} \tau_{a5} + i_{a5} \tau_{a1}}{2} \right) \cos 4\theta \right\} \\ &= T_{A0} + T_{Ripple} + T_{\xi} \end{aligned} \quad (3-8)$$

where  $T_{A0}$  is the torque component that contributes to useful torque and it is set such that  $T_{A0} = T_L /$  with  $T_L$  being the load torque and  $T_{Ripple}$  the ripple torque component that constitutes to no useful torque.  $T_{\xi}$  is the torque component that reduces to zero with the summation of corresponding torque components from B-phase and C-phase torques.

The optimal excitation for a given load torque,  $T_L$ , is the current excitation that will give a minimum copper loss. Therefore, the parameter to be minimized is:

$$P_{loss} = \frac{1}{2} (i_{a1}^2 + i_{a5}^2) R \quad (3-9)$$

and by substituting the eqn. (3-8) into eqn (3-9), and differentiating it with respect to  $i_{a1}$ , the optimal current excitation or the identity current components are given by

$$i_{a1} = \frac{4}{\tau_{a1}^2 + \tau_{a5}^2} T_{A0} \tau_{a1} \quad \& \quad i_{a5} = \frac{4}{\tau_{a1}^2 + \tau_{a5}^2} T_{A0} \tau_{a5} \quad (3-10)$$

Eqn. (3-9) shows the two current components that form the identity current. In a current controlled motor drive, the current  $i_a$  can be generated and controlled by fast power electronics and be fed to the motor. This is applicable to current-controlled drives as described in reference [4]. However, as all the drivers for the spindle motor are usually voltage-controlled instead of current controlled, it is necessary to determine the input voltage characteristics that will provide the identity current.

### 3.4 Voltage-controlled Spindle Drive

Conventional spindle motor drive uses six-step voltage input. The 120° duty cycle voltage waveform is used.

In contrast, a variable duty-cycle voltage waveform shown in Fig.2 is proposed. By controlling the angles  $\gamma$  and  $\phi$ , it is expected that the identity current can be produced and fed to the motor. Using Fourier analysis, this variable duty-cycle voltage can be written as:

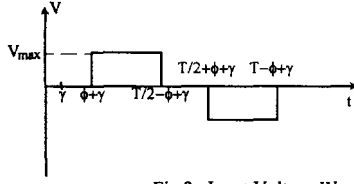


Fig 2. Input Voltage Waveform

$$v_a' = \sum_{n=0, n=3k}^{\infty} v_{asn} \sin n\theta + v_{asn} \cos n\theta$$

where

$$v_{asn} = \frac{8V_d}{n2\pi} \cos n\omega\phi \cos n\omega\gamma$$

$$v_{asn} = -\frac{8V_d}{n2\pi} \cos n\omega\phi \sin n\omega\gamma \quad (4-1)$$

Using the expression for voltage in eqn (2-7) and eqn (3-10), the voltage equation is rewritten as :

$$v_a = (i_{a1}R + \tau_{a1}\omega) \sin \theta + (i_{a5}R + \tau_{a5}\omega) \sin 5\theta + \omega(L - M)(i_{a1} \cos \theta + i_{a5} \cos 5\theta) \quad (4-2)$$

Taking only the fundamental and fifth harmonic components of eqn.(4-1) and equating it with eqn.(4-2),

$$\frac{8V_d}{2\pi} \cos \omega\phi \cos \omega\gamma = i_{a1}R + \tau_{a1}\omega \quad (4-3)$$

$$-\frac{8V_d}{2\pi} \cos \omega\phi \sin \omega\gamma = i_{a1}\omega(L - M) \quad (4-4)$$

$$\frac{8V_d}{10\pi} \cos 5\omega\phi \cos 5\omega\gamma = i_{a5}R + \tau_{a5}\omega \quad (4-5)$$

Several parameters from eqns (4-3) to (4-5) are needed to form the solutions for identity current. These are,

- $V_d$  - input dc link voltage
- $\phi$  - duty cycle control angle (sec)
- $\gamma$  - load angle (sec)

To solve for these parameters, the problem is formulated as an optimization problem. The objective function to be minimized is given by

$$\mathfrak{J}(V_d, \phi, \gamma) = v_a' - v_a$$

where  $v_a'$  is the voltage in eqn. (4-1) and  $v_a$  is the voltage in eqn. (4-2). In the optimization, following practical constrains are imposed :

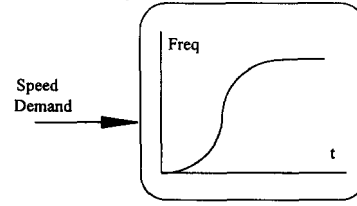
- C1:  $V_{max} - V_d \geq 0$   
to limit the link voltage to a manageable max value
- C2:  $\frac{\pi}{2} - \phi \geq 0$   
to reduce pulse to zero or negative width if  $\phi \geq \frac{\pi}{2}$
- C3:  $\frac{2\pi}{\omega_r} - \gamma \geq 0$   
 $\gamma$  is periodic with period  $\frac{2\pi}{\omega_r}$

The above problem is a constrained optimization problem. Some penalty functions are used to transform the problem into an unconstrained one, and the simplex method used for solution of the resulting unconstrained problem. The voltage pattern that will produce the required identity current is thus determined.

#### 4. OPEN LOOP FREQUENCY CONTROL

The spindle motors in HDDs are conventionally self-starting and operating without sensors in BLDCM mode. Alternatively self-starting and sensorless operations can be achieved by using an open-loop frequency control technique, whereby the input current frequency is ramped up from low frequency to a synchronous frequency. The motor is started at a low frequency for the rotor to track the rotating field, and thus achieving the self-starting operation. Subsequently the motor speed will be ramped to and maintained at the desired synchronous speed. This method has been applied in the control of synchronous motor [5].

The profile of the input frequency to self-start the spindle motor is shown in Fig. 3. A S-curve is used due to its desirable features. The S-curve is divided into three periods. In the first period, the ramping of the frequency is slow for the motor to pick up speed. When the motor picks up speed, the frequency is ramped up more rapidly. This is the second period. Approaching the synchronous speed, the input frequency has to be slowed down until synchronous speed is achieved.



Input Frequency  
Fig 3 Starting S-Curve

Operating as a synchronous motor the speed will subject the motor to fluctuate due to torque pulsation. As it is operating in the open-loop mode, it is susceptible to disturbances such that shock and vibrations. This problem is addressed in Section 7.

#### 5. SIMULATION

##### 5.1 Electromagnetic and Mechanical Subsystems

Simulations on the identity control technique and the open loop frequency operation are carried out and compared with the conventional sensorless BLDCM spindle drive. In these simulation the power converter is considered perfect and loseless.

The motor identity of the torque profile for the phase-A winding is obtained experimentally and it is shown in Fig. 4. Fourier analysis of the identity shows that the 3rd harmonic is indeed negligible as compared to the fundamental and 5th harmonics, thus validating the assumption made in the analysis in section 3. This motor identity is analyzed and used in the simulations and experiments.

The parameters of the hard-disk spindle motor and its operating conditions are also measured and given in Table 1.

Using the above parameters and analysis in Sections 3 and 4, the identity current components as in eqn (3-10) are found to be

$$i_{a1} = 0.1275 \text{ \& } i_{a5} = -0.01136$$

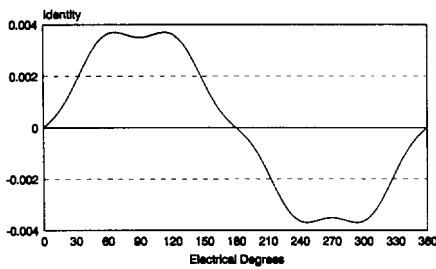


Fig. 4 Motor Identity Obtained experimentally

Resistance, R	6.59Ω
Inductance, L-M	0.878mH
Identity	$a = 3.856 \times 10^{-3} \sin \theta$ $- 0.3436 \times 10^{-3} \sin 5\theta$ Nm/A
Load Torque, $T_L$	2.229 mNm
Speed	3600 rpm

Table 1. Hard-Disk Parameters and Operating Conditions

### 5.2 Optimization Parameters

As detailed in the Section 4, optimization has to be performed to determine few optimal operating conditions for the drive. Using penalty functions and simplex method, the voltage excitation to achieve the identity current above is :

$$V_d = 8.84, \phi = 22.4^\circ, \gamma = -1.5^\circ$$

### 5.3 Open-loop Frequency Control

An experimental study of the motor responses to various starting frequency was performed and the optimal input frequency profile for accelerating the motor to the synchronous frequency is determined. The S-curve is determined quantitatively as in Fig. 3 and used in the simulations

### 5.4 Speed Response

The identity controlled and open-loop frequency controller with the parameters above was simulated using SIMNON in the open-loop frequency control mode. The speed response is given in Fig 5.

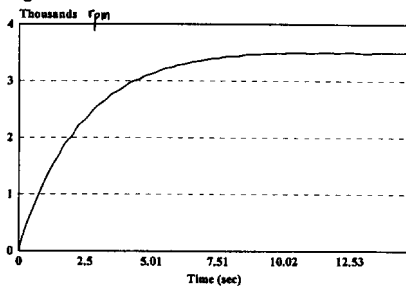


Fig 5. Speed Response

The simulated results show good speed response. The speed gets steady at around 8 s, which is reasonable specification for HDDs. The speed deviation at steady state is within  $\pm 1$  rpm, which is considered good at present standard.

### 5.5 Comparison of Performance of Identity Current and Ideal Rectangular Current

The effectiveness of the identity control coupled with open-loop frequency control scheme is compared with a conventional BLDCM mode operated on the same motor. The BLDCM control mode uses three-phase six-step excitation. The voltage in this case will have a pulse-width of 120°. The simulation assumes that the motor has zero inductance.

In this simulation, the parameters for the drive using identity control and open-loop frequency starting technique are found to be :

$$\begin{aligned} i_{a1} &= 0.12 \text{ A} & i_{a5} &= -0.10 \text{ A} \\ V_{\max} &= 4.67 \text{ V} \end{aligned}$$

The conventional controller uses 12 V dc link voltage. The efficiencies for both controller are as follows :

Conventional Controller	- 78.10%
Identity Controller	- 83.85%

It is obvious that there is a significant improvement in the efficiency of the drive system using new controller. A reason for this improvement is due to the production of useful torque (positive sequence torque) by the harmonics injected in the motor using identity control. in the BLDCM mode control the current harmonics produce negative sequence torque and as a result it requires a larger fundamental current to sustain the load torque. A larger motor loss is thus incurred and the efficiency drops. This is further elaborated in Section 7.

### 6 QUASI-RESONANT CONVERTER

The switching power converter for the spindle drive in the hard-disk is another critical component of the system. Presently PWM and linear systems are used and the switching loss in PWM systems can be excessive due to the simultaneous presence of a high current and a high voltage during turn-on and turn-off periods. Recent development in power electronics has shown that by adding a high-frequency resonant circuit around the switch, it is possible to shape the switching current and voltage waveforms so that a high current and voltage are not present at the same time during the turn-on or turn-off periods. This technique, which combines the PWM and resonant techniques, is referred to as the *quasi-resonant* technique [6]. The resonant circuit can be connected to the switch to eliminate either the turn-off or turn-on switching loss. There are a few circuit topologies available for implementation, and in this paper the zero voltage switching (ZVS) topology is used due to its ease of implementation and reduced number of component count. It eliminates the turn-on loss by turning on the switch when the voltage is zero [7]. The topology implemented for the spindle drives in this paper is described in reference [6] and it is shown in Fig. 6.

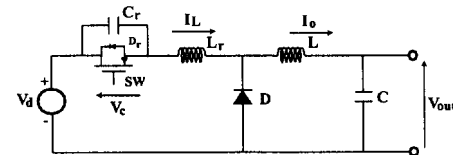


Fig 6. Buck ZVS QRC

### 7. HARDWARE IMPLEMENTATION

Hardware for identity control, open-loop frequency technique and buck ZVS-QRC is implemented and the block diagram is as shown in Fig. 7. This implementation drives a 3.5" HDD spindle motor which has the motor parameters listed in Table 1.

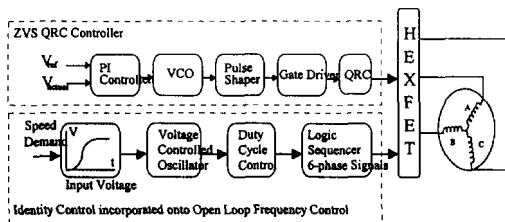


Figure 7. Block Diagram Of Hardware Implementation

### 7.1 ZVS-QRC Implementation and Results

The following components values are used for ZVS :

$C_r$	-	9 nF	$L_r$	-	100 $\mu$ H
SW	-	IRF630	D	-	1N4001
L	-	100 $\mu$ H	C	-	470 $\mu$ F

Figs 8 and 9 show the experimental waveforms of the ZVS-QRC with the motor acting as the load drawing a current of 109 mA at 9.05 V. Using a NMOS as the switch, the switching on and off of the switch are denoted by the positive going transition and negative transition of the gate signal respectively. It is observed that the switching occurs when the voltage across the switch is zero. This shows that the zero voltage switching is achieved.

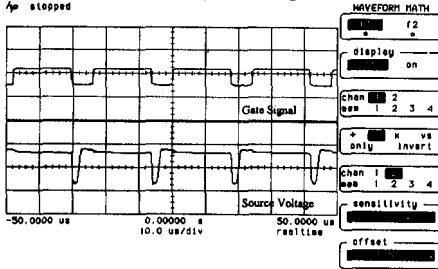


Fig 8. Gate Signal Waveform With Respect To Source Voltage

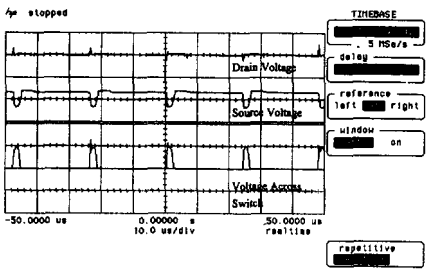


Fig 9. Voltage Across Switch With Respect To Source Voltage

The efficiency of the QRC was measured and tabulated in Table 2. The efficiency is computed using the following equation :

$$\eta = \frac{V_{out}^2 R}{V_i I_i}$$

The input voltage to the converter is set at 12.0V and for the test, the output voltage is set on open loop and uncontrolled.

By averaging the efficiencies for the various resistive loads, an average efficiency of 83.9% was achieved. Similarly, with the motor acting as the load (as shown in last row in Table 4, motor running at 3600 rpm), the efficiency of the converter was found to be 82.5%.

Input Current (mA) $I_i$	Output Voltage (V), $V_{out}$	Load ( $\Omega$ )	Efficiency (%), $\eta$
130.1	8.20	56.0	76.4
92.1	9.57	100.0	82.9
65.9	10.13	150.0	86.5
47.7	10.64	220.0	89.9
107.2	9.04	(Motor Load)	82.5

Table 2. Experimental Data For QRC

### 7.2 Performance Comparison with BLDCM Control

A hardware system for motor drive which comprises the open-loop frequency starting technique, ZVS-QRC and identity control technique is developed. Experiments are carried out by driving a 3.5" HDD spindle motor. Another similar set of experiment is also carried out using a conventional drive system. The performance of the both drive systems are compared.

The following figures, Fig. 10 and Fig. 11, show the typical phase current and back emf waveforms for both the identity controller and conventional BLDCM controller.

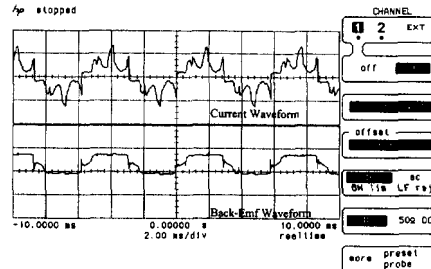


Fig. 10 Phase current and back emf waveforms for the identity controller

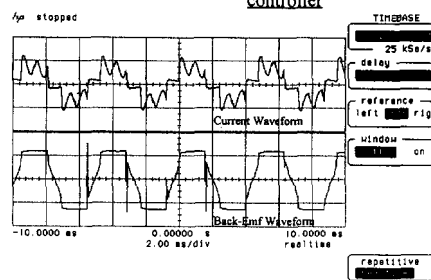


Fig. 11 Phase current and back emf waveforms for conventional BLDCM controller.

It is observed that the currents for both controllers are different from the theoretically assumed rectangular currents. This is due to the non-rectangular back-emf of the motors. To further analyze the results, with the drive at 3600 rpm, the waveforms were recorded and Fourier analyzed. Several sets of readings were taken and tabulated in Table 3.

The experimental results show that the fundamental current of the conventional controller is larger than that for the identity controller. The fifth harmonic of the BLDCM drive controller is positive in sign while that of the identity controller is negative in

	Identity Current	Conventional Current
Fundamental	0.1308	0.1336
Second	-0.0023	-0.0007
Third	0.0006	-0.0015
Fourth	-0.00004	0.0019
Fifth	-0.0278	0.0604
Sixth	-0.0008	0.0024
Seventh	0.0457	0.04938
Eighth	-0.0007	0.00226

Table 3. Current Harmonics Of Both Controllers

sign. This difference in sign accounts for the higher fundamental current in the conventional spindle drive controller. Since the fifth harmonic in the identity is negative in sign, it generates a positive sequence torque while the positive fifth current harmonic of the conventional drive system will produce a negative sequence torque. Hence, a larger fundamental current is necessary for the conventional system to sustain the same load torque.

Table 4. shows the efficiencies obtained from the tests with the spindles running at 3600 rpm.

Identity Controller		
Input Power	Motor Losses	Efficiency
0.479	0.081	83.15%
0.480	0.082	82.92%
0.481	0.082	82.91%
0.488	0.084	82.82%
<b>Overall Efficiency</b>		<b>82.95%</b>

Conventional Controller		
Input Power	Motor Losses	Efficiency
0.548	0.131	76.08%
0.542	0.132	75.56%
0.529	0.121	77.06%
0.525	0.113	78.44%
<b>Overall Efficiency</b>		<b>76.79%</b>

Table 4. Power Distribution For Both Controllers

The efficiency of the motor with identity control is better by an average of 6%.

The performance of the controller was also compared in terms of its steady speed accuracy and robustness. Both controllers were able to maintain a speed of 3600 rpm with a speed deviation of  $\pm 1$ rpm. However, the open loop frequency control, though having the advantage of simplicity in implementation and its ability to self start, suffers in terms of robustness compared to the BLDCM drive with position feedback. The open loop frequency controller is unable to handle persistent disturbances due to the absence of feedback. Nevertheless it is applicable in disk drive systems as the load torque in disk drive applications are nearly constant throughout the whole operation. Tests on the open loop controller by subjecting the drive to reasonable disturbances, such as intermittent contact of the disk with the head carried by the VCM, show that the spindle is able to maintain its rotation at the constant speed.

## 8. CONCLUSIONS

A new spindle motor drive system which incorporates the following features has been implemented :

- Identity Control
- Self-Starting
- Sensorless Operation
- Quasi Resonant Converter

Simulations and hardware implementation for the new drive system were carried out and the results were compared with the conventional HDD spindle motor driver. The results showed that the new controller performed better than the conventional one in certain aspects such as the power efficiency, speed regulation and torque ripple requirement. Future works however is required to improve the robustness of the new drive system.

## LIST OF REFERENCES

- [1] Philips Data Book, *Application Notes for BLDCM Driver TDA 5140*.
- [2] T. J. E. Miller, *Brushless Permanent-Magnet and Reluctance Motor Drives*, Clarendon Press, Oxford, 1989.
- [3] Bi Chao, Chang Kuan-Teck and Low Teck-Seng, *Method and Apparatus for Establishing a Reference Current for Use in Operating a Synchronous Motor*, US Patent Pending.
- [4] Yew Wen Ching, *Identity Control for Permanent-Magnet Synchronous Motors*, B.Eng. Thesis, Dept of Electrical Engineering, NUS, 1993.
- [5] J. M. D. Murphy and F. G. Turnbull, *Power Electronics Control of AC Motors*, Pergamon Press, 1988.
- [6] Wojciech A. Tabisz, Pawel M. Gradzki, and Fred C. Y. Lee, *Zero Voltage Quasi-Resonant Buck Converters*, IEEE Trans. Power Electron., vol. 4, No. 2, pp. 194- 203, 1989.
- [7] Kwang-Hwa Liu and Fred C. Y. Lee, *Zero Voltage Switching Technique in DC/DC Converters*, IEEE Trans. Power Electron., vol. 5, No. 3, pp 292- 304, 1990.